Management of ambiguities in magnetostratigraphic correlation

F. Lallier, C. Antoine, J. Charreau, G. Caumon, J. Ruiu

Management of ambiguities in magnetostratigraphic correlation[☆]

Florent Lallier[a,b,*], Christophe Antoine[b], Julien Charreau[c], Guillaume Caumon[a], Jeremy Ruiu[a,b]

[a] *Georessources (UMR 7359 CNRS, Université de Lorraine-ENSG), 2 rue du Doyen M. Roubault, 54500 Vandoeuvre lès Nancy, France*
[b] *ASGA, rue du Doyen Marcel Roubault, 54500 Vandoeuvre lès Nancy, France*
[c] *CRPG (UMR 7358 CNRS, Université de Lorraine-ENSG), 15 rue Notre Dame des Pauvres, 54500 Vandoeuvre lès Nancy, France*

Abstract

Magnetostratigraphy is a powerful tool to provide absolute dating of sediments enabling robust and detailed chronostratigraphic correlations. It is based on the correlation of a magnetic polarity column, observed and measured in a given sediment section, to a magnetic polarity reference scale where polarity changes are well dated *via* other independent methods. However, magnetostratigraphic correlations are loose as they are only constrained by binary magnetic chrons (*i.e* normal or reversal) and their thickness, which are both defined from depth variations of the magnetic remanent directions. The thickness of a given magnetic polarity zone is a function of time and sediment accumulation rate, which may not be stationary, leading to ambiguities when performing the correlations.
To address these ambiguities, a numerical method based on the Dynamic Time Warping algorithm is proposed. Magnetostratigraphic correlations are computed in order to minimise the local variation of the accumulation rate. The main advantage of the proposed method is to automatically provide a set of reasonably likely correlations. This set can then be scrutinised for further analysis and interpretation. However, the likelihood of a correlation should be handled carefully as it depends on the information content of the magnetostratigraphic section itself and remain ultimately valid by ancillary constraint. Nevertheless, the method gives consistent results on difficult synthetic cases that simulate abrupt variations of the sedimentation rate. Insights on true sections debated by previous authors are also given.

Keywords: magnetostratigraphy, computer method, uncertainty

Introduction

Sedimentary basins provide key records of many earth processes including tectonic, climatic and erosional. They may also host large resources of ore deposits (e.g gold, U, etc.), hydrocarbons and fresh water. Accurate and detailed chronostratigraphy is critical to yield quantitative constraints on the wide variety of interactions that may exist between these processes. This observation holds for reservoir and basin modeling which are also based on stratigraphic correlation and request reliable chronology. Sediment dating is therefore a fundamental step for a broad community in Earth sciences. Various techniques have been developed such as radio-isotopic dating (e.g K-Ar, Fission Tracks), biostratigraphy, cosmonucleid isotopes (10Be / 26Al), astronomical records, palynology, 14C, varves *etc.* All these methods enable the dating of sediments in a large range of environments and for time scales ranging from years to 10^7 years. However, in continental areas, due to the paucity of biostratigraphic markers, reliable dating via classic methods remains challenging. Hence, the depositional ages are mainly inferred from loose lithostratigraphic correlation, which suffers from flaws in the presence of strong lateral facies variations and diachronous deposition (e.g. Charreau et al. (2009b)).Yet, continental sediments may record the Earth magnetic field and its polarity at the time of deposition via the Detrital Remanent Magnetization (DRM) mechanism (e.g Tauxe et al. (2006)). Given a sedimentary section or a log, one can measure the variation of the remanent magnetic directions and identify the polarity changes of the Earth magnetic field. A polarity column can then be reconstructed as a succession of polarity zones (or reversal) characterised by their length in meters or duration in years and their polarity (normal or reverse). A normal polarity chron is represented in black in a polarity column and corresponds to a period where the Earth magnetic dipole is similar to the present one with the magnetic North close to the geographic North. A reverse polarity chron is shown in white and corresponds to a period where the dipole has been switched with its magnetic North close to the southern Earth's pole.
Magnetostratigraphy is based on the correlation of a measured polarity column in a sediment section with the geomagnetic polarity time scales (GPTS (Lourens et al., 2004)), where polarity changes are well dated via independent methods (astronomical constraints, spreading of the oceanic floor, thermochronology). This powerful technique enables the dating of sediments in many areas where other approaches have failed. However, magnetostratigraphy is based on several assumptions: (1) the Earth magnetic field is bipolar; (2) the sedimentary section is con-

[☆]Published in Earth and Planetary Science Letters 371-372 (2013)26–36, doi:10.1016/j.epsl.2013.04.019; Code available from server at `http://www.gocad.org/w4/index.php/research/free-software`.

[*]Corresponding author
Email addresses: `lallier@gocad.org` (Florent Lallier), `antoine@gocad.org` (Christophe Antoine), `charreau@crpg.cnrs-nancy.fr` (Julien Charreau), `Guillaume.Caumon@univ-lorraine.fr` (Guillaume Caumon), `ruiu@gocad.org` (Jeremy Ruiu)

tinuous with no depositional hiatus nor erosion; and (3) the accumulation rates are constant at short time scales (< few Ma). This method is particularly well suited for the Cenozoic Era and Jurassic Period in which numerous polarity changes have been documented.
Nevertheless, the major drawback of this dating technique is that the correlation between the observed polarity column and the reference scale is a subjective and qualitative interpretation as only based on eyes, providing a single dating with no assessment of uncertainty. Other datings, for example from fossil or lava flows observed in the studied section, are therefore very useful to independently constrain the correlation and reduce uncertainty. In many cases, the absence of such data leads to controversial debates between authors leaving magnetostratigraphic correlation results to doubts and criticism. For example in the Subei section in Western China, three different authors have proposed different correlations with ages ranging between 33.5 and 27 Ma (Yin et al., 2002), 26 and 19 Ma (Gilder et al., 2001), and 20 and 9 Ma (Wang et al., 2003), leading to conflicting interpretations about the tectonoclimatic history of the Northeast Tibet Plateau (section 2.1).
A magnetic polarity column only provides a partial view of the sedimentary record. It is therefore almost impossible to find "the right" correlation model, as to do so would require a huge amount of independent data impossible to acquire in practice. Instead, we suggest to automatically generate possible correlation models by using well-established rules and principles in order to deal with uncertainty. In the proposed algorithm (section 1.3.1), each correlation is associated with a cost, which is used to rank the various proposed solutions according to specified rules. Moreover, the proposed approach provides an estimate on the instantaneous accumulation rate and their uncertainties on the basis of several possible solutions while classic "eye-based" correlation only gives the 90-95% confidence limit from basic linear regression built on a unique correlation.
Tests carried out on synthetic polarity columns (Section 1.4) attest that the algorithm can handle sedimentary hiatus and sharp variations of the accumulation rate. The method is therefore applied to the Subei and Yaha magnetostratigraphic sections in Central Asia (section 2) where a debate still remains on the depositional ages although they represent standard sections for tectonics and climate in this region. The analysis of the 10,000 minimum cost correlations, covering many acceptable possibilities for these sections provides interesting insights about the correlations discussed in the literature.

1. Computer method for magnetostratigraphic correlation

1.1. Problem Settings

Computing correlations between magnetic polarity section and polarity reference scale is challenging since:(*i*) the magnetic record is binary information (*ii*) the studied section represents only a part of the whole polarity reference scale and has potentially been transformed by changes in the accumulation and compaction rates and (*iii*) undersampling may yield unrecorded polarity changes.
Moreover, in a sedimentary section, the correlation to the reference scale strongly depends on the thickness of each polarity zone, which is a function of three parameters : (*i*) the duration of the polarity chrons $i(t)$; (*ii*) the accumulation rate $p(t)$ and (*iii*) the compaction rate c. From a mathematical analysis, Lowrie and Kent (2004) show that the geomagnetic polarity time serie is not stationary but is composed of stationary periods. They also reveal that the duration of the polarity chrons follows a Poisson law. The accumulation rate is also a non-stationary process as it is driven by the nature of the depositional environment and erosion processes, which may rapidly (i.e. few kyr) and strongly varies. However, authors often consider the accumulation rate to change stepwise between long stationary periods. For example, from magnetostratigraphic study of the Jingou He section in northern Tianshan piedmont, Charreau et al. (2009a) found that the mean accumulation rate was 0.10 mm/yr, 0.18mm/yr and 0.29mm/yr from 23 Ma to 16Ma, from 16Ma to 11Ma and from 11Ma to 1Ma, respectively. Finally, the compaction rate may vary along a given section due to rock lithology and burial leading to distortion of the observed accumulation rate.
To provide robust, relevant and trustworthy correlations, computer based methods will be required to handle distortion in the time signal of the magnetic chrons induced by these processes (accumulation rate, compaction rate...).

1.2. Previous work

Man (2011) proposes an interesting computer method which correlates a given polarity column to the reference scale under the following assumptions: (*i*) the thickness of the observed polarity zone is supposed stationary, (*ii*) the polarity column is supposed complete (all polarity changes have been recorded and sampled in the section), (*iii*) the age of the studied column is *a priori* roughly known and (*iv*) the geomagnetic reversal process is supposed to follow a Gaussian law. As pointed out above, these assumptions can be discussed when working on long sedimentary sections. First, the chron thickness and duration are mainly non-stationary. Second, due to non-depositional and/or erosional periods, several magnetic polarity changes may be missed in the sediment record. Moreover, non-amenable lithology for sampling (e.g conglomerate) may sometimes impose low sampling density insufficient to identify all magnetic reversals. And finally, in continental areas it is sometimes very difficult to assess the age of a given section from sedimentology only, due to the absence of biostratigraphic markers. For example, in Central Asia, thick conglomerate lying at the top of the basin sedimentary piles, have long been assigned to the Plio-pleistocene whereas recent magnetostratigraphic studies have shown that their deposition could start during the middle Miocene (Charreau et al., 2009).
Another way to correlate a given polarity column to the reference scale was proposed by Man (2008). This method is based on a preprocessing step which transforms both the polarity column and the reference scale to dimensionless data by calculating the logarithm of the thickness (or the duration) of a given magnetic chron minus the loga-

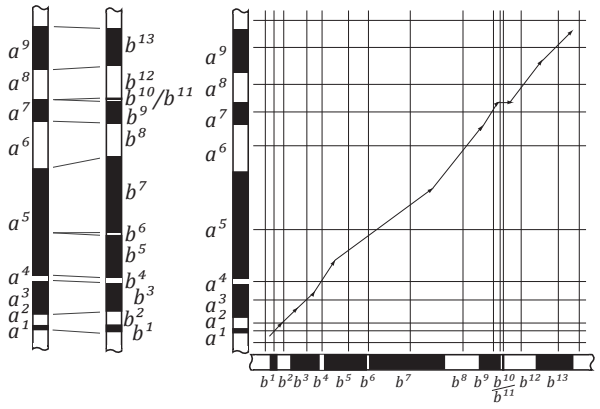

Figure 1: Correlation between two polarity columns and associated correlation path in the DTW table displaying gaps (chrons b^{10} and b^{11}) and "one to many correlation" (chrons a^5, b^5, b^6 and b^7)

rithm of the thickness (or the duration) of the underlying chron. Thanks to this transformation, accumulation rate and chron duration can be supposed locally stationary. The correlation between the reference scale and the studied polarity column is then computed using a cross correlation function. This method is less sensitive to the non-stationarity of the data but still requires that all reversals have been recorded and sampled in the sediments. In this paper, we similarly use thickness ratios to relax the global assumption of stationary preservation rate.

1.3. Proposed approach

Our approach has been designed to manage non-stationary data, unrecorded chrons in the polarity column (sedimentary hiatus and/or erosion) and to support independent constraints derived from biostratigraphy or geochemical dating techniques. This method is based on the Dynamic Time Warping (DTW) algorithm described in section 1.3.1 (Levenshteiti, 1966). The DTW algorithm is modified to output not only the "*best*" correlation between the studied polarity column and the GPTS, but also the "*n best*" correlations in order to manage uncertainties on sediment dating and accumulation rate. The Python implementation used in this paper is available at the address `http://www.gocad.org/w4/index.php/research/free-software`, at which new versions will be posted. Input data are: (*i*) the reference polarity section which is supposed exhaustive (i.e. there is no polarity change in the recorded section which is not in the reference scale); (*ii*) the thickness of polarity zones observed in the sediment section.

1.3.1. The Dynamic Time Warping algorithm

The Dynamic Time Warping (DTW) algorithm has been introduced by Levenshteiti (1966) and found many applications for automatic signal correlation in speech recognition (Myers and Rabiner, 1981), bioinformatic and geoscience for the correlation of magnetic susceptibility stratigraphic sections (Hladil et al., 2010), lithostratigraphic correlation (Smith and Waterman, 1980) or for the correlation of well logs (Fang et al., 1992). Lisiecki and Lisiecki (2002) propose to correlate paleoclimate record using a dynamic programming method comparable to the DTW algorithm.

Consider two columns **a** and **b** presented in Fig.1, composed of polarity zones noted from a^1 to a^9 and chrons noted from b^1 to b^{13}, respectively. The correlation between the two columns can be represented as a path $CP(\mathbf{a},\mathbf{b}) = [cp_1,\ldots,cp_i,\ldots,cp_k]$ in a $2D$ diagram (Fig.1) where cp_i is an element of the path. In the example presented in Fig. 1 $CP(\mathbf{a},\mathbf{b})$ is noted:

cp_1	cp_2	cp_3	cp_4	cp_5	cp_6	cp_7	cp_8	cp_9	cp_{10}	cp_{11}
a^1	a^2	a^3	a^4	a^5	a^6	a^7	$\emptyset$	$\emptyset$	a^8	a^9
b^1	b^2	b^3	b^4	$b^5\ b^6\ b^7$	b^8	b^9	b^{10}	b^{11}	b^{12}	b^{13}

Four different configurations may arise: (1) two units are well correlated (i.e. diagonal arrow in the diagram noted $cp_i = (a^f, b^g)$; (2) a polarity zone in column **a** is missing in column **b** (i.e. vertical arrow noted $cp_i = (a^f, \emptyset)$); (3) a polarity chron in column **b** is missing in column **a** (i.e. a horizontal arrow noted $cp_i = (\emptyset, b^g)$); and (4) a polarity zone of **a** (respectively **b**) is associated to several polarity chrons of **b** (respectively **a**, see the correlation of chrons a^5 in Fig. 1). This last configuration will be addressed in section 1.3.2.
A cost is associated to each of these first three configurations. The best correlation between the two columns is the one for which the sum of the individual costs of all successive configurations is minimal. The cost of the correlation $CP(a_i, b_j)$ between column **a** from a^1 to a^i and column **b** from b^1 to b^j, $C(i,j)$ is recursively computed as follows:

$$C\left(a^i, b^j\right) = \min \begin{bmatrix} c(a^i, b^j) + C\left(a^{i-1}, b^{j-1}\right) \\ g(a^i) + C\left(a^{i-1}, b^j\right) \\ g(b^i) + C\left(a^i, b^{j-1}\right) \end{bmatrix} \quad (1)$$

where $c(a^i, b^j)$ is the cost of a correlation (called a match and noted $cp_l = (a_i, b_j)$) between two units and $g(a^i)$ and $g(b^i)$ are the costs of an extra unit (called a gap) in column **a** (noted $cp_l = (a_i, \emptyset)$) and column **b** (noted $cp_l = (\emptyset, b_j)$), respectively. Applying Eq. (1) from $i = 1$ to 9 and $j = 1$ to 13 yields the minimum cost correlation between columns **a** and **b**.

1.3.2. Specification to magnetostratigraphy

In the following section, we present how the DTW algorithm has been improved in order to achieve correlations between a given magnetic polarity column and the GPTS. Let **a** denote the polarity column established from paleomagnetic sampling and analyses, and **b** the polarity reference scale.

Cost computation We first assume that the reference scale **b** is complete, meaning that each polarity change a^i recorded in the polarity column **a** must be correlated to a polarity change in the reference scale **b**. Therefore, we set the cost of a gap in the studied polarity column to be equal to the infinity: $g(a^i) = \infty$.
The cost $c(a^i, b^j)$ of a match between a polarity chron (of the reference scale **b**) and a polarity zone (of the polarity column **a**), is considered only if the two considered units have the same polarity. Moreover, the cost of a match is designed to minimise local variations of the accumulation rate.

Let $t(a^i)$ refer to the thickness, in meters, of the i^{th} polarity zone recorded in the studied polarity column, $p(a^i)$ its polarity, $d(b^j)$ the duration of the j^{th} polarity chron of the reference scale and $p(b^j)$ its polarity. When the correlation between a^i and b^j is evaluated within the DTW algorithm, the correlation $CP(a^{i-1}, b^{j-1})$ is known. Let u and v be the last two units correlated before a^i and b^j:

$$\begin{array}{c} CP(a^{i-k}, b^{j-l}) = [cp_1, \ldots, cp_k] \\ (u, v) = cp_{k-l} \text{ where } u, v \neq \emptyset \\ \text{with } l \text{ as close as possible to 1} \end{array} \quad (2)$$

The match cost between a^i and b^j, is defined by:

$$\begin{array}{lll} \textbf{if } p(a^i) \neq p(b^j) & c(a^i, b^j) = \infty & \\ \textbf{else} & c(a^i, b^j) = \left(r^1/r^2\right) - 1 & \text{if } r^1/r^2 > 1 \\ & c(a^i, b^j) = \left(r^2/r^1\right) - 1 & \text{if not.} \\ \text{where,} & r^1 = t(a^i)/d(b^j) & \\ \text{and,} & r^2 = t(u)/d(v) & \end{array} \quad (3)$$

The use of a ratio in the cost function ensures that compared values are dimensionless. This cost function can be computed under the assumption that the accumulation rate is locally stationary in the two considered chrons. Due to discrete sampling, the thickness of a polarity zone in the studied section is not exactly known. Moreover, error is proportionally more important for thin polarity zones than for large ones. Uncertainty on the thickness of small polarity zones is managed by multiplying the match function by a correction factor $k(a^i)$:

$$k(a^i) = 0.8 \times log\left(1 + \frac{min\left(t(a^i), t(a^{i-1})\right)}{\bar{t}(\mathbf{a})}\right) \quad (4)$$

where $\bar{t}(\mathbf{a})$ is the mean thickness of polarity zones on the studied section.

The cost of a gap in the reference scale $g(b^j)$ is computed as the ratio between the duration of the considered chron $d(b^j)$ and the mean duration of chrons of the reference scale $\bar{d}(\mathbf{b})$. It corresponds to the cost of an unsampled, non-recorded (i.e non-deposition) or eroded polarity zone on the polarity column. It is therefore computed as $g(b^j) = d(b^j)/2\bar{d}(\mathbf{b})$ and respects the intuitive idea that non-sampled or non-preserved polarity zones are preferentially the smallest ones.

Gap management Most of the time, when a polarity change has not been sampled or preserved in the sediments, the resulting polarity column may display a polarity interval which actually includes two or more chrons of the reference scale (see correlation between chrons a^5 and b^5, b^6 and b^7 in Fig.1). Waterman and Raymond Jr. (1987) introduce the "one to many matching" possibility in the DTW algorithm. In this case, one unit of a column may be correlated to several units of the second column. However, assuming that the magnetic polarity reference scale is complete implies that the "one to many matching" can only occur in one way, between one polarity zone of the studied polarity column and several chrons of the reference scale. Let $mg\left(a^i, [b^{j-1}, b^j, b^{j+1}]\right)$ denote the cost of a "one to many match" between polarity zone a^i of the polarity column and chrons b^{j-1}, b^j and b^{j+1} of the reference scale. If the polarity of a^i, b^{j-1} and $b^j + 1$ are the same, the "one to many" correlation is considered and

$$\begin{array}{c} mg\left(a^i, [b^{j-1}, b^j, b^{j+1}]\right) = c(a^i, b^{j-1,j+1}) + g(b^j) \\ \text{where } b^{j-1,j+1} \text{ is a chron with a duration} \\ d\left(b^{j-1,j+1}\right) = d(b^{j-1}) + d(b^{j+1}). \end{array} \quad (5)$$

Management of borders A given polarity column observed in a sediment section contains only few units with respect to the reference scale. Therefore, in the DTW algorithm many gaps should arise at the polarity column extremities (Fig.2). Let's consider a polarity column **a** with its first polarity zone called a^1 and its last called a^n to be correlated to the reference scale noted **b**. As proposed by Smith and Waterman (1980) these extremities issues are managed by setting $g(b^j) = 0$ in Eq.1 if $i = 1$ or $i = n$.

Constraining the correlation using independent dating Some additional dating information derived from biostratigraphy (*e.g.* Charreau et al. (2009a); Sen et al. (1986)), cosmonucleid isotopes (*e.g.* Hu et al. (2011)), palinology (*e.g.* Dupont-Nivet et al. (2008)), *etc.*, may enable to independently constrain the ages of a stratigraphic section. However, such independent age constraints will only be valid at a specific stratigraphic depth. Let $a^{i\star}$ be the i^{th} polarity zone of the polarity column where one has independently dated the sediment between 15 and $18Ma$ (Fig.2). The matching cost function is thus transformed to $c(a^{i\star,b^j}) = \infty$ if polarity chron b^j is older than $18Ma$ or younger than $15Ma$. This ensures that polarity zone $a^i\star$ is correlated to reference chrons dated between 15 and $18Ma$.

Best and n-best correlations Within the DTW algorithm, the cost of a match between a given polarity zone and a chrons (a^i and b^j) must be calculated independently from the correlation of the other units ($CP(a^{i-1}, b^{j-1})$). Our matching function (Eq.3) does not respect this condition. Therefore, to ensure the finding of the minimum cost correlation $CP(\mathbf{a}, \mathbf{b})$, the DTW algorithm is modified to output the k correlations $[CP(a^i, b^j)]^k$ between a^1 to a^i and b^1 to b^j built from modified version of equation 1:

$$\left[C\left(a^i, b^j\right)\right]^k = \min^{\mathrm{k}} \begin{bmatrix} c(a^i, b^j) + \left[C\left(a^{i-1}, b^{j-1}\right)\right]^k \\ g(a^i) + \left[C\left(a^{i-1}, b^j\right)\right]^k \\ g(b^i) + \left[C\left(a^i, b^{j-1}\right)\right]^k \end{bmatrix} \quad (6)$$

where $\left[C\left(a^i, b^j\right)\right]^k$ are costs associated to the k correlations $\left[C\left(a^i, b^j\right)\right]^k$.

Tests carried out on various polarity columns show that if k is large enough, the optimal correlation is found (for example $k > 1,000$ ensures finding the minimum cost correlation between a polarity column of 25 polarity zone and a GPTS of 290 chrons).

Furthermore, this new version of the DTW algorithm computes not only the minimum cost correlation but also the n best correlations of a polarity column, offering insight into uncertainty in dating and accumulation rates estimation. As for the minimum cost correlation, a number k of

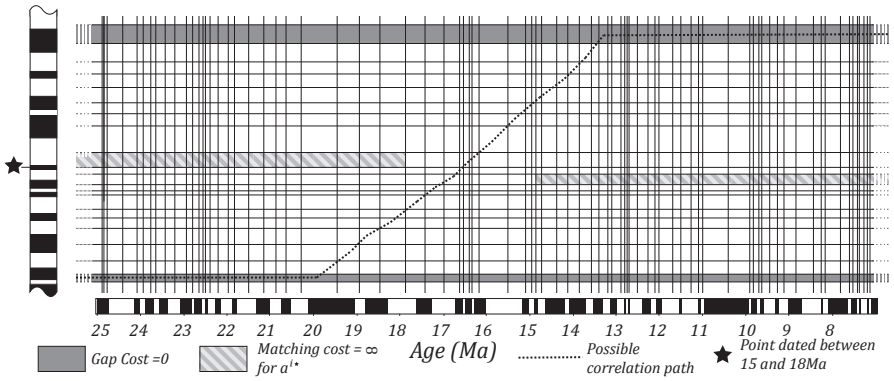

Figure 2: DTW table for correlation between a polarity column (vertical) and the polarity reference scale (horizontal). Cells on which matching and gap costs are computed to manage extremities of the polarity column are displayed in dark grey. Cells on which matching and gap costs are computed to constrain correlation with dated point of the polarity column are displayed in light grey.

computed correlations should be large enough to ensure finding the n minimum cost ones ($k > 20,000$ correlations are output to obtain the $n = 10,000$ minimum cost one in example presented in section 1.4).
Tests carried out on synthetic data sets (columns of 7 polarity zones are correlated to a 25 polarity chrons reference scale) where all possible correlations can be computed (125,423 in this case) show that the correlation costs follow an exponential distribution for the better half of the correlation. In a basic magnetostratigraphic problem (a 25 units polarity column to correlate to a reference scale covering the past 150My, *i.e.* 290 polarity chrons) the number of possible correlations reaches 10^{30} which is technically impossible to compute. Therefore only a few percent of the possible correlations can be done which we call the n best correlations. As presented above, $k > n$ correlations should be computed to ensure finding the n best correlations. If k is too low, the costs distribution does not exhibit an exponential distribution, indicating that the n output correlations do not represent the real n minimum cost ones. k can then be increased until the cost histogram honours the exponential function for realisation 1 to n.

Statistical analysis of the n best correlations The relationship between the cost of a correlation and its rank, considering only the n best (n being low when compared to the total number of possible correlation) could be modelled by:

$$[CP(\mathbf{a},\mathbf{b})]^m \simeq \frac{1}{k_1} ln\left(k_2 \times m + k_1^{[CP(\mathbf{a},\mathbf{b})]^0}\right) \qquad (7)$$

where, k_1 and k_2 are two constants greater than one, and $[CP(\mathbf{a},\mathbf{b})]^m$ is the cost of the m$^{\text{th}}$ best correlation. The cost-rank function computed for the study of the Xishuigou section (section 2.2h) is presented in Fig. 4. Two groups of correlations can be identified on the rank-cost function: (i) a first group, corresponding to the first hundred correlations in which the correlation cost increases rapidly with the rank; (ii) a second group, called cost plateau, where the cost gently increases with the rank. Tests carried out on short synthetic polarity columns show that the second group actually includes about half of the entire possible correlations. We define "interesting correlations" as the correlations with a cost close to the minimum one and which therefore can be considered as likely. The first group actually corresponds to this definition of "interesting correlation".

Analysing the n best correlations of a polarity column offers an insight into uncertainties on sediment dating and resulting conclusions (accumulation rate, ...). A statistical analysis of uncertainty in a magnetostratigraphic study requires a number n of correlations large enough to ensure that all interesting correlations has been output. A qualitative evidence that all "interesting correlations" have been considered is the presence of a plateau for the cost-rank function (*e.g.* as observed in Fig. 4h).

Visualization of the n best correlations A visual and intuitive representation of the possible correlations (10,000 for the magnetostratigraphic column we studied) is a useful tool for the understanding of magnetostratigraphic uncertainties. Here, we propose a visualisation method of the n best correlations based on a representation of the dating weighted density. For each polarity zone a^i of the studied polarity column, its mean age is computed on each of the n best correlations $[CP(a^i, b^j)]^n$ and plotted on a depth-time diagram. We propose the contribution w_i of each dating $CP_i(\mathbf{a},\mathbf{b})$ to be inversely proportional to its cost $C_i(a,b)$:

$$w_i = 1 - \frac{C_1(\mathbf{a},\mathbf{b}) - C_i(\mathbf{a},\mathbf{b})}{C_1(\mathbf{a},\mathbf{b}) - C_n(\mathbf{a},\mathbf{b})} \qquad (8)$$

A kernel smoother (Wand and Jones, 1995) is then applied to this set of weighted points, resulting in a representation of the alternative correlations where their relative probability is represented by the normalised weighted density map (Fig.3).

1.4. Validation of the proposed approach

The proposed approach is tested on two synthetic polarity columns designed to evaluate how non-stationary accumulation rate, erosion, faulting events and incomplete sampling are managed by the algorithm.

Synthetic column description A first synthetic polarity column (Fig.3 A) is built from the GTPS using

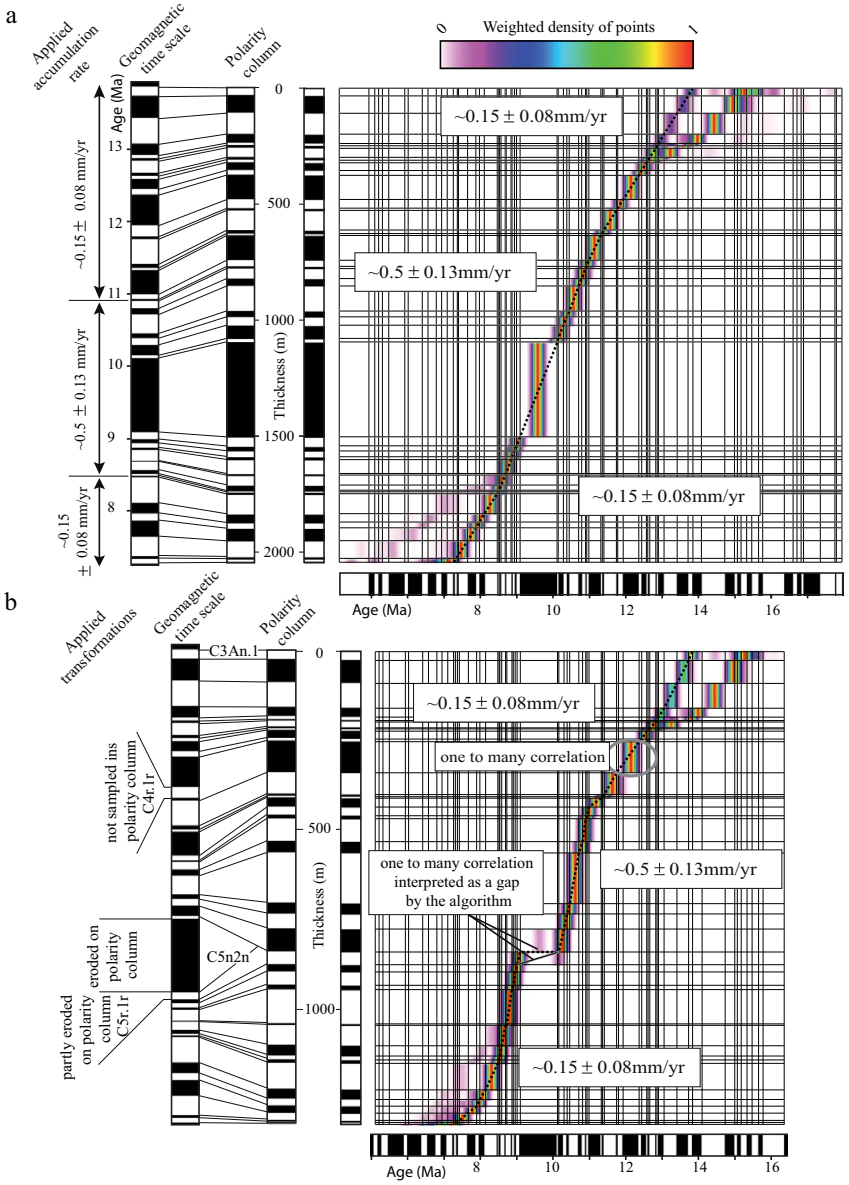

Figure 3: Correlation test with a polarity column where accumulation rate is not stationary (A) and where some polarity zones are not sampled or eroded (B). Dashed lines correspond to the minimum cost correlation of each case.

a non-stationary and non-constant accumulation rate between polarity chrons *C3A.2n* to *C5Ar.2r*. Chrons *C3An.2n* to *C4Ar.1r** and *C4Ar.1r** to *C5r.3r-1n* were modified using accumulation rates drawn independently from a distribution law U $[0.06, 0.23]$ mm/yr while chrons *C5r.3r-1n* to *C5Ar.2r* were modified using a law U $[0.37, 0.63]$ mm/yr. The second synthetic polarity column (Fig.3 B) is designed to check whether or not our method enables us to manage un-sampled, eroded or faulted polarity zones. Two modifications are made on the first synthetic polarity column: (i) the reverse chron *C4r.1r* is suppressed, resulting in a normal polarity zone with a thickness equal to the cumulated thickness of polarity zones *C4n.2n*, *C4r.1r* and *C4r.1n*; (ii) a gap of up to 1Ma is added by "eroding" completely the chron *C5n.2n* and partially the chron *C5r.1r* yielding a reverse polarity zone with a thickness equal to the thickness of chron *C5n.1r* and the remaining part of *C5r.1r*.

Result analysis Correlation results can be analysed via the minimum cost correlation (dash line in Fig.3) but also using the statistical distribution of the n best correlations.

Minimum cost correlation

The minimum cost correlation computed on the first synthetic column exactly reproduces the expected correlation. These results show that our correlation method manages non-stationary sediment accumulation rates. The correlation computed on the second synthetic polarity column is consistent with the way we built it. The un-sampled polarity chron (*C4r.1r*) is well recognised by the algorithm and results in a one to many correlation in the DTW table. The erosion occurring in chrons *C5n.2n* and *C5r.1r*

is partially well identified. Contrary to a one to many correlation (*i.e.* chons c of the polarity column correlated with *C4r.1r*, *C5n.1r* and *C5n.2n*), the algorithm outputs an erosion of chron *C5n.1r* and *C5n.2n*.

N best correlations

The probability density plot of the 10,000 best correlations of the two synthetic polarity columns are presented in Fig. 3. The quality of the resulting solutions is similar for the two columns. Dating of the central part of the polarity column (from 300m to 1600m and from 250m to 1000m for the first (Fig.3a) and the second polarity column (Fig.3b)) does not display major variation around the minimum cost correlation and attests a good confidence on the given ages in this part. At the point where the result of a faulting event has been mimicked in the second synthetic polarity column, variations arise around the minimum cost correlation, suggesting a possible missing polarity zone. Two other variations appear at the top of both polarity columns. In a real case, these variations may lead to alternative interpretations in terms of accumulation rates as presented in section 3.

2. Application to recent magnetostratigraphic analyses in Central Asia

2.1. Central Asia a key area for tectonics, climate and resources in Asia

Central Asia is constituted by several large and very active mountain ranges including the Tianshan, the Qilianshan, the Kunlun Shan, *etc.* All these ranges dominate the topography over thousands of metres with some summits higher than 7km. While originally formed during a long-lived Paleozoic to Mesozoic history of subduction/collision of several continental blocks (*e.g.* Windley et al. (1990)), their high present topography attests to an intense and younger deformation: all these ranges were uplifted and reactivated under the India-Asia collision (Tapponnier and Molnar, 1979). Therefore, since the collision started 55Ma ago (Patriat and Achache, 1984), this region has played a key role during the deformation of the Asian continent accommodating up to 40% of the whole convergence between India and Asia. Moreover, intense deformation and tectonics in this area has probably strongly impacted the Asian and global climate, yielding a strong aridification of Central Asia (Fluteau et al., 1999). The material eroded and shed from these uplifting mountains fills several large intracontinental basins (Tarim, Qaidam, Junggar) where thick and continuous sedimentary deposits have recorded tectonic and climate changes. Thanks to numerous tectonic wedges and large river entrenchments, thick and continuous sedimentary sections are now well exposed at the toes of these mountain ranges, enabling the analyses of sediments for tectonics, climate change, natural resources, textitetc. However, due to their continental origin, these sediments are poorly dated *via* classic biostratigraphic method, which greatly inhibits our ability to stratigraphically correlate different sections or to place temporal bound on tectonic and climate processes. Therefore during the past decades, magnetostratigraphy has been the technique of choice to better constrain the depositional ages of these series and numerous studies have been published in international journals. However, subjective magnetostratigraphic correlations sometimes yield controversial ages because several authors may propose several correlations for the same section. Consequently, the interpretation and conclusions derived from these controversial ages are open to debate. Two examples of conflicting interpretation will be discussed and treated below.

2.2. The Xishuigou section

The Xishuigou section is located in NE Tibet in the Subei area. In this section three authors have proposed three different magnetostratigraphic correlations yielding depositional ages that vary by about 20Ma. Gilder et al. (2001) first dated the section between 26Ma and 19Ma (Fig.4) while later Yin et al. (2002) correlated the same section from 33.5 to 27, and Wang et al. (2003) from 20 to 9Ma. These contrasting results are very puzzling as they lead to conflicting interpretations. It is nevertheless very important to better assess the depositional ages in this section as they bear on tectonics and climate change linked to the NE Tibet uplift.

We first output the 10,000 minimum cost correlations considering all magnetic polarity changes identified in Gilder et al.'s first column. Output correlations are presented in Fig. 5. The minimum cost correlation dates the Gilder et al.'s column from reference polarity chron *C5n.1n* to *C5Er* which is equivalent to the age proposed by Wang et al. (2003). This also holds for the 10 best ones. The first solution equivalent to Gilder et al.'s interpretation is the 1171st with a cost of 10.33 and a weight of 0.27, which do not let it appear in the weighted density plot. Based on the correlation rules described above, this interpretation may thus be interpreted as improbable. The solution proposed by Yin et al. (2002) does not appear in the 10,000 minimum cost correlations output. The analyses of the density plot show two alternative solutions of the top of the polarity column. The most probable one indicates an accumulation rate decrease at ca. 13 Ma.

When looking at differences between our computed correlations and the interpretation proposed by Wang et al. (2003) it appears that: (i) we found no faulting event as interpreted by Wang et al. (2003) at polarity zone g; (ii) in our results, 12 polarity chrons are missing which represent about 50% of the whole reference chrons for the considered period. Given the sampling density, this is unlikely. Such a large discrepancy may suggest that unknown events in the reference scale may have been identified in the Gilder et al's column as suggested by these authors (Gilder et al., 2001). Therefore, we performed a second test where short polarity zones b and 11 supported by only two paleomagnetic samples are not considered. Results presented in Fig. 4c show that the minimum cost correlation (with a cost of 6.67) is then exactly the same as the interpretation proposed by Gilder et al. (2001). The 10 best correlations are also in the same range of age. The first output correlation comparable to the interpretation proposed by Wang et al. (2003) is the 248th one with a cost of 7.94998. The weighted age density plot shows that the two alternative correlations proposed by Gilder et al. (2001) are the most

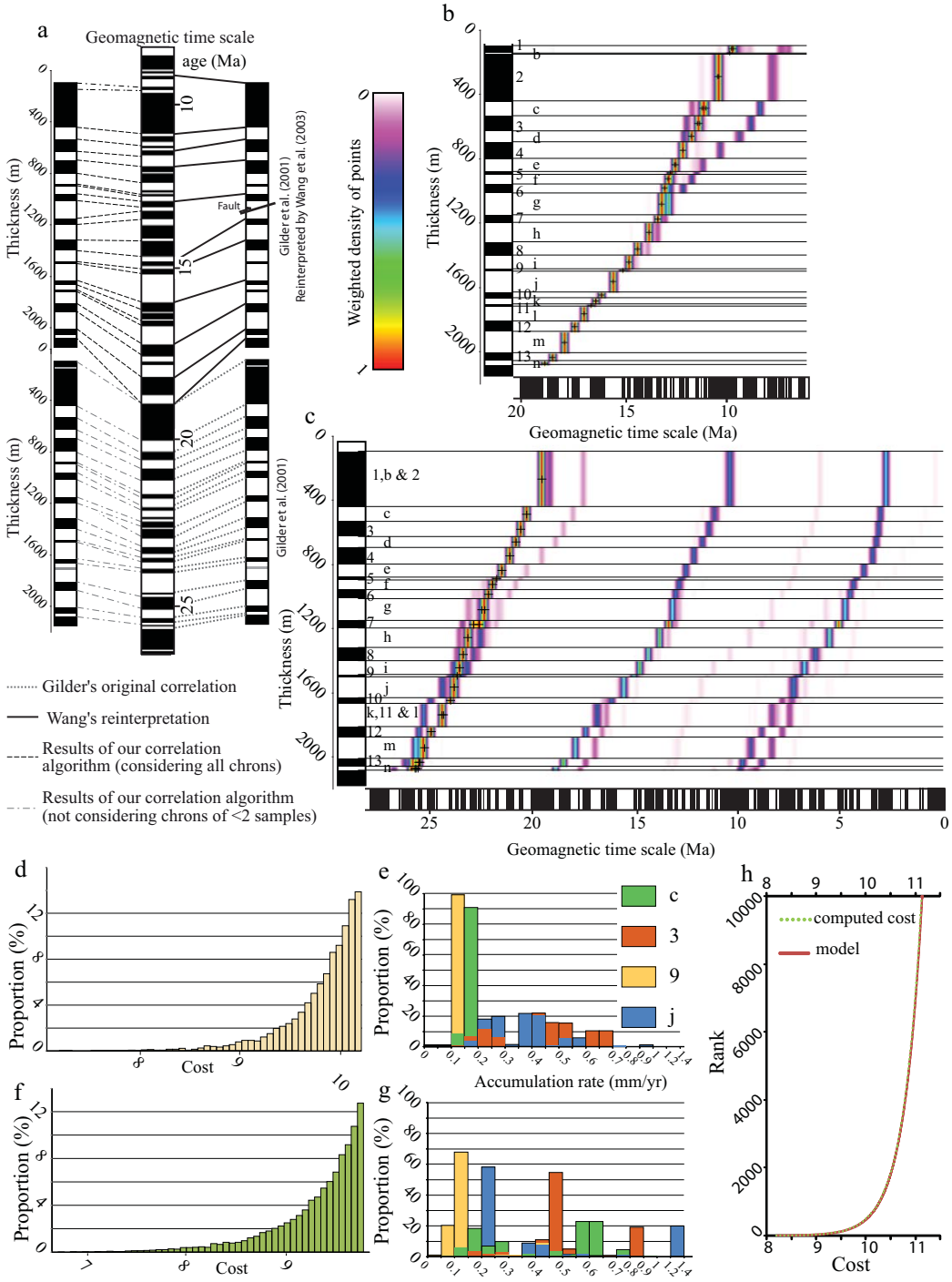

Figure 4: Correlation results for the Xishuigou section. (a)Comparison between correlation proposed by Gilder et al. (2001), (Wang et al., 2003) and minimum cost correlation computed considering all polarity changes sampled by Gilder et al. (2001) and only polarity zones supported by more than 2 samples. (b) and (c) weighted density age versus depth plot of the 10,000 bests correlations computed considering all polarity zones (b) and only polarity zones supported by at least two samples (c). (d) and (e), related cost distribution for the 10,000 best correlations. (e) and (g) related weighted accumulation rate distribution at polarity zones c, 3, 9 and j. (h) cost-rank function for the 10,000 best correlations considering all sampled polarity changes. The proposed model is computed thanks to equation 7 with $k_1 = ln(14.7)$ and $k2 = 10^9$.

probable. Then two other groups of probable alternative solutions appears: one group corresponding to the interpretation proposed by Wang et al. (2003) and one between 2.5 Ma et 10 Ma. The solution proposed by Yin et al. (2002) is not reproduced in the computed 10,000 best correlations.
From these results we conclude that, when loose polarity zones b and 11 are removed, the most probable correlation dates the section from chrons *C6n* to *C7Ar**. Although the correlation proposed Wang et al. (2003) remains possible, no faulting event seems to be justified in the absence of other observation.

2.3. The Yaha section

In the Yaha section located in southern Tianshan, two authors also have proposed different correlations with the reference scale. Charreau et al. (2006) established the first magnetostratigraphic column which they correlated to the reference scale from 12.5 to 5.2Ma and, later, thanks to complementary sampling above the first section, from 12.5 to 1.7Ma (Charreau et al., 2009b). The sedimentation rates derived from this correlation show a stepwise acceleration at 11Ma which authors relate to enhanced uplift in the Tianshan mountains. Huang et al. (2006) challenge this view and correlate Charreau et al's first bottom section from 9 to 2Ma which yields accelerated sedimentation rates at 7Ma, concluding that the Tianshan underwent intense deformation at this time. Despite some clues indicating that Huang's proposition was probably invalid (Charreau et al., 2008) and the fact that the upper section has been sampled since, the debate may remain open. The approach presented here enables us to decipher which correlation is the most probable following rules described in section 1.3 (fig.5). The analysis of the 10,000 best correlations confirms the interpretation proposed by Charreau et al. (2009b). The minimum cost correlation faithfully reproduces Charreau et al's correlation with a small variation on the top on the polarity column and the 10,000 best correlations all show an accumulation rate acceleration between 10 and 11 Ma.

3. Certainty and uncertainty on sediments age and accumulation rates

3.1. Magnetostratigraphic data and correlation confidence

Evaluating the degree of confidence in a given magnetostratigraphic correlation is critical. It depends on the sampling density and the uncertainty degree of the polarity column correlation to the GPTS.
The sampling density and its ability to ensure identification of all the polarity zones recorded in the studied section can be evaluated via s jackknife test (Tauxe and Gallet, 1991).
Uncertainty about the correlation mainly originates from: (i) the number of recorded magnetic polarity zones in the studied section and (ii) the distortion of the recorded signal. For example, a succession of three polarity zones may correlate to many parts of the GPTS while a column of fifty polarity zones, recorded in sediment deposited under constant accumulation rate, will yield a unique dating solution. In contrast, non-stationary accumulation rate, faulting event, erosion, *etc.* may lead to complex polarity columns that are difficult to correlate to the GPTS. A significant problem in magnetostratigraphy is to evaluate whether the information content of a section is sufficient to date rocks with enough confidence. From the set of realisations, a possible criterion for evaluating this aspect could be to look at the spread for the age of each polarity zone (e.g., standard deviation, interquartile range) or the number of modes of the age distribution for each polarity zone. Taking the average over all polarity zones of age standard deviations or interquartiles as a criterion seems a viable way to assess the significance of the correlations. For example, 10,000 realisations of a three- polarity zones section would undoubtedly yield a very large average age spread, meaning that we don't have enough information to deduce anything. Data are in this case considered as non-informative. Conversely, for a longer section, this average dispersion should decrease. An argument against such a procedure is that the method forces alternative solutions to be considered, hence artificially increases the spread when the number of realisations is large. However, as pointed out in Section 1.3.2 the correlation cost reaches a plateau when the number of computed correlations is high. Hence the weight (Eq.8) of unlikely realisations tends to zero. The use of the weighted standard deviation allows computing a factor characterising the capability of a column to provide dating with confidence. The weighted standard deviation for a given polarity zone sd_w^c is defined by:

$$sd_w^2 = N' \times \frac{\sum_{i=1}^{N} w_i \times (x_i - \bar{x_w})^2}{(N'-1) \times \sum_{i=1}^{N} w_i} \tag{9}$$

where N is the number of realisations, N' the number of realisations with a non-zero weight w_i, x_i the age of the polarity zone and $\bar{x_w}$ the mean age of the polarity zone considering the N realisations. The mean value of the weighted standard deviation $\bar{sd}_w$ can be computed considering all polarity zones of the considered column. Following results are obtained for the Xishuigou section and the Yaha section:

- $sd_w^c = 0.03Ma$ for the Yaha section (Fig.5b).
- $sd_w^c = 0.72Ma$ for the Subei section considering all sampled reversals (Fig. 4b).
- $sd_w^c = 7.82Ma$ for the Subei section considering only the polarity zones supported by at least 2 samples (Fig. 4d).

A high sd_w^c suggests that the data available for the magnetostratigraphic correlation are non-informative and thus that additional data coming from other dating methods (*e.g.*, palynology, cosmogenics) should be used to better constrain the correlation.

3.2. Sampling bias and accumulation rate uncertainty

From detailed accumulation rates, one may quantify subsidence, sedimentary fluxes (*e.g.* Métivier et al. (1999)) or reconstruct past erosion rates (*e.g.* Charreau et al. (2011)). Evaluating the uncertainty on accumulation rates is therefore critical to better manage these calculations. Even in the Yaha section, though good confidence exists

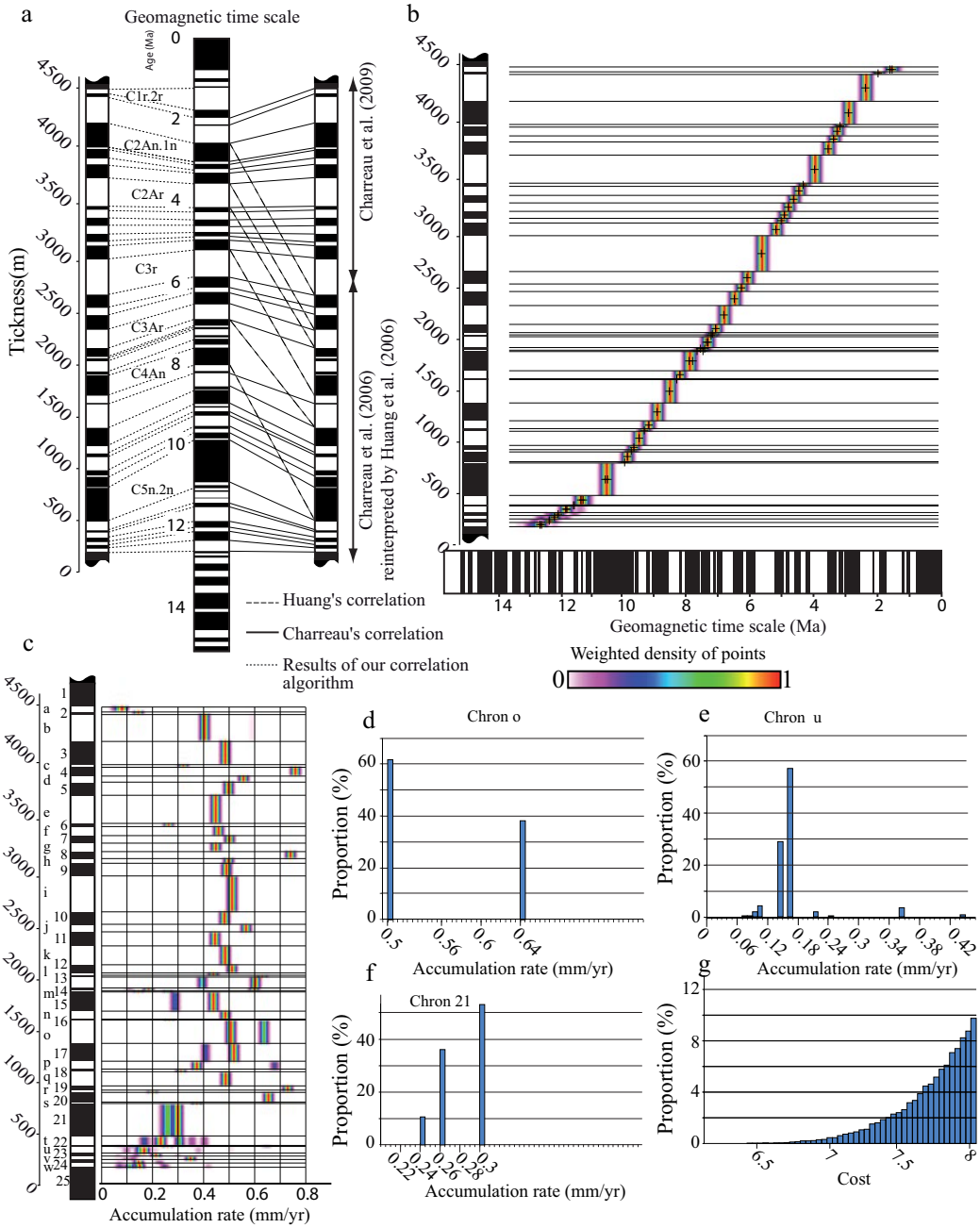

Figure 5: Magnetostratigraphic correlation of the Yaha section. (a) Comparison between correlation proposed by Charreau et al. (2009b), Huang et al. (2006) and the minimum cost correlation. (b) Weighted density age versus depth plot of the 10,000 bests correlations. (c) Weighted density plot of instantaneous accumulation rate. (d), (e) and (f) Histogram of accumulation rates weighted by correlation cost for polarity zones o, u and 21. (g) Cost distribution of the 10,000 bests correlations.

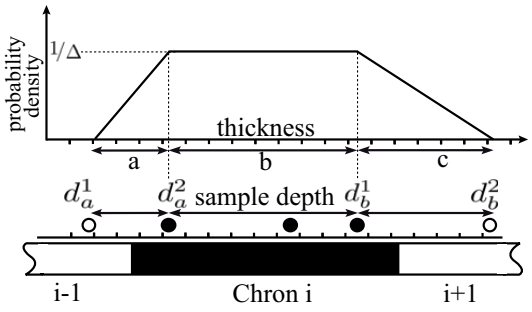

Figure 6: Thichness probability density function $t(x)$ of polarity zone i computed from depth of samples d_a^1, d_b^1, d_a^2, and d_b^2 and distance separating these samples a, b and c.

on the correlation to the GPTS, significant uncertainties on instantaneous accumulation rates remain. Fig. 5c displays a weighted density plot of instantaneous accumulation rates, computed as the depth-time density plot (see section 1.3.2) from the 10,000 best correlations of the Yaha polarity column to the GPTS. Figs. 5d, e and f presents the histogram of accumulation rate calculated for polarity zones o, u and 21 respectively, calculated for each of the 10,000 correlations and weighted by each correlation cost. From these diagrams, it turns out that the accumulation rate is most uncertain for the bottom part of the polarity column where multimodal distributions are observed (polarity zones 21 to w). For example, in polarity zone u, it ranges between 0.07 mm/yr and 0.35 mm/yr, with a mode of 0.16 mm/yr. Accumulation rates calculated for polarity zone 21 are comprised between 0.24 mm/yr and 0.3 mm/yr. Above, the uncertainty decreases with accumulation rates varying between 0.5 and 0.64 mm/yr for polarity zone o.

The observed instantaneous accumulation rate is dependent on the thickness assigned to a polarity zone. Since the thickness of a given polarity zone is derived from the depth variation of the magnetic direction, discrete sampling should also yield the uncertainty on the exact position of the magnetic polarity change. This uncertainty could be quantified. Let d_a^1 and d_b^1 denote the depth of two successive samples of opposite magnetic orientation between which lies one of the two limits of the considered polarity zone is and d_a^2 and d_b^2 the depth of the two samples defining the second limit of the polarity zone. We note $\Delta = max(|d_a^1 - d_b^1|, |d_a^2 - d_b^2|)$ and $\delta = min(|d_a^1 - d_b^1|, |d_a^2 - d_b^2|)$. The probability density function of the polarity zone thickness $t(x)$ (Fig. 6) may be taken as:

$$t(x) = \begin{pmatrix} 0 \text{ if } x < |d_b^1 - d_a^2| \\ 0 \text{ if } x > |d_a^1 - d_b^2| \\ x - d_a^2 + d_b^1/\Delta \cdot \delta \text{ if } x \in \left[|d_b^1 - d_a^2|, |d_b^1 - d_a^2 + \delta|\right] \\ 1/\Delta \text{ if } \text{ if } x \in \left[|d_b^1 - d_a^2 + \delta|, |d_b^1 - d_a^2 + \Delta|\right] \\ -x - d_a^1 - d_b^2/\Delta \cdot \delta \text{ if } x \in \left[|d_b^1 - d_a^2 + \Delta|, |d_a^1 - d_b^2|\right] \end{pmatrix} \quad (10)$$

Errors on polarity zone thickness have a particular impact on the instantaneous accumulation rates computed on thin polarity zones. Examples of its impact can be observed on Fig. 5c where abrupt variation of the accumulation rate on thin polarity zone (c, 4, 6 and 8 for instance) are questionable. In those cases, the thickness probability density function should be used to better evaluate uncertainties on accumulation rates. Moreover, uncertainty on polarity zone thickness could also impact the dating. The corrective cost computed thanks to equation 4 allows us to handle uncertainty on polarity zone thickness. However it does not take into account the probability density function of polarity zone thickness and thus does not allow propagating it down to the accumulation rate. A way to propagate the polarity zone thickness uncertainty down to the accumulation rate would be: (i)build n polarity columns sampling possible thicknesses of each polarity zone; (ii) correlate the n columns to the GPTS using the proposed approach; (iii) compute weighted age and accumulation rate density plots from the correlations of the n columns. However, this approach, based on a simple sampling of the polarity zone thickness, requires generating and correlating a substantial number of polarity columns and is not applicable in practice. Additional research is thus required to develop an optimised methodology.

Other sources of uncertainty in sediment dating and accumulation rate estimation come from the GTPS itself. Agrinier et al. (1999) proposed a probabilistic representation of chron age in the GPTS. This representation should be used to incorporate GPTS uncertainty on sediment dating. However, we consider that this uncertainty is low as compared to bias induced by the non-stationary accumulation rate, fault, erosion and sampling strategy and, to a lesser extent, sediment compaction rate.

Conclusion

This paper introduces a new method for correlating a given magnetostratigraphic column to the GPTS with systematic and explicit rules (or cost function, see section 1.3.2). Uncertainties on magnetostratigraphic correlations interpreted by geologists come from characteristics of the sedimentary record (accumulation variability, fault or erosion) but also from the subjectivity of such an interpretation. The proposed numerical approach does not claim to be objective, because correlation rules proposed in section 1 are also subjective. However these correlation rules are explicitly and mathematically expressed and can be discussed, whereas a handmade correlation cannot be evaluated without additional external constraints on the age of rocks (such as fossil, pollen fission track ...) .

The two main improvements of our method are: (i) its ability to handle, in the stratigraphic record, potential gaps either due to non sampling, sedimentary hiatus (non-deposition and/or erosion) or faulting and non-stationary and variability of sediment accumulation; (ii) the possibility to compute and analyse not only the most probable correlation but also the n best correlations of a section.

The main flaw of our technique is that we assume all polarity changes recorded in a studied sedimentary section are known in the GPTS. In particular cases, when short term polarity zone or local sediment re-magnetisation occurs, this limitation may represent obstacle to a good correlation. However, such debatable polarity zones are supported only by a few samples and represent thin polarity zone on the sedimentary section. Since our correlation method manages gaps well, debatable polarity zones could be ignored in the correlation computation and thus automatically managed by adding a gap if they are actually

identified in the GPTS.

The proposed correlation method offers a different approach to magnetostratigraphic studies. A large view of possible correlations of a given polarity column can be computed in a short amount of time (about 2 hours for the Yaha section when the entire GPTS is considered). A statistical study of sediment deposition age and related accumulation rate is thus possible. Moreover, the method can shed new light on hand made deterministic correlations by providing alternative solutions.

Acknowledgements

This work was performed in the frame of the GOCAD research project. The companies and universities members of the GOCAD consortium (www.gocad.org) are acknowledged for their support. Tom Blanchard, Stuart Gilder and two anonymous reviewers are acknowledged for their valuable suggestions for improving this paper. This is CRPG contribution number 2236.

Agrinier, P., Gallet, Y., Lewin, E., 1999. On the age calibration of the geomagnetic polarity timescale. Geophysical Journal International 137 (1), 81–90.

Charreau, J., Blard, P.-H., Puchol, N., Avouac, J.-P., Lallier-Vergs, E., Bourls, D., Braucher, R., Gallaud, A., Finkel, R., Jolivet, M., Chen, Y., Roy, P., 2011. Paleo-erosion rates in Central Asia since 9Ma: A transient increase at the onset of Quaternary glaciations? Earth and Planetary Science Letters 304 (1-2), 85–92.

Charreau, J., Chen, Y., Gilder, S., Barier, L., 2008. Comment on "Magnetostratigraphic study of the Kuche depression, Tarim Basin, and Cenozoic uplift of the Tian Shan Range, Western China" Baochun Huang, John D.A. Piper, Shoutao Peng, Tao Liu, Zhong Li, Qingchen Wang, Rixiang Zhu [Earth Planet. Sci. Lett., 2006, doi:10.1016/j.epsl.2006.09.020]. Earth and Planetary Science Letters 268 (3-4), 325–329.

Charreau, J., Chen, Y., Gilder, S., Barrier, L., Dominguez, S., Augier, R., Sen, S., Avouac, J.-P., Gallaud, A., Graveleau, F., Wang, Q., 2009a. Neogene uplift of the Tian Shan Mountains observed in the magnetic record of the Jingou River section (northwest China). Tectonics 28 (2).

Charreau, J., Gilder, S., Chen, Y., Dominguez, S., Avouac, J.-P., Sen, S., Jolivet, M., Li, Y., Wang, W., 2006. Magnetostratigraphy of the Yaha section, Tarim Basin (China): 11 Ma acceleration in erosion and uplift of the Tian Shan mountains. Geology 34 (3), 181–184.

Charreau, J., Gumiaux, C., Avouac, J.-P., Augier, R., Chen, Y., Barrier, L., Gilder, S., Dominguez, S., Charles, N., Wang, Q., 2009b. The Neogene Xiyu Formation, a diachronous prograding gravel wedge at front of the Tianshan: Climatic and tectonic implications. Earth and Planetary Science Letters 287 (3-4), 298–310.

Dupont-Nivet, G., Hoom, C., Konert, M., 2008. Tibetan uplift prior to the eocene-oligocene climate transition: Evidence from pollen analysis of the xining basin. Geology 36 (12), 987–990.

Fang, J. H., Chen, H. C., Shultz, A. W., Mahmoud, W., 1992. Computer-aided well log correlation. American Association of Petroleum Geologists Bulletin 76 (3), 307–317.

Fluteau, F., Ramstein, G., Besse, J., 1999. Simulating the evolution of the asian and african monsoons during the past 30 myr using an atmospheric general circulation model. Journal of Geophysical Research D: Atmospheres 104 (D10), 11995–12018.

Gilder, S., Chen, Y., Sen, S., 2001. Oligo-Miocene magnetostratigraphy and rock magnetism of the Xishuigou section, Subei (Gansu Province, western China) and implications for shallow inclinations in central Asia. Journal of Geophysical Research B: Solid Earth 106 (B12), 30505–30521.

Hladil, J., Vondra, M., Cejchan, P., Vich, R., Koptikova, L., Slavik, L., 2010. The dynamic time-warping approach to comparison of magnetic-susceptibility logs and application to Lower Devonian calciturbidites (Prague Synform, Bohemian Massif). Geologica Belgica 13 (4), 385–406.

Hu, X., Kirby, E., Pan, B., Granger, D. E., Su, H., 2011. Cosmogenic burial ages reveal sediment reservoir dynamics along the yellow river, china. Geology 39 (9), 839–842.

Huang, B., Piper, J., Peng, S., Liu, T., Li, Z., Wang, Q., Zhu, R., 2006. Magnetostratigraphic study of the Kuche Depression, Tarim Basin, and Cenozoic uplift of the Tian Shan Range, Western China. Earth and Planetary Science Letters 251 (3-4), 346–364.

Levenshteiti, V., 1966. Binary codes capable of correcting deletions, insertions, and reversals. In: Soviet Physics-Doklady. Vol. 10.

Lisiecki, L., Lisiecki, P., 2002. Application of dynamic programming to the correlation of paleoclimate records. Paleoceanography 17 (4), 1049.

Lourens, L., Hilgen, F. J., Shackleton, N. J., Laskar, J., Wilson, J., 2004. Orbital tuning calibrations and conversions for the Neogene Period. In: Gradstein, F., Ogg, J., Smith, A. (Eds.), A Geologic Time Scale 2004. Cambridge University Press, Cambridge, pp. 469–471.

Lowrie, W., Kent, D., 2004. Geomagnetic polarity timescales and reversal frequency regimes. In: Channell, J., Kent, D., Lowrie, W., Meert, J. (Eds.), Timescales of the Paleomagnetic Field. AGU Geophysical Monograph Series 145, pp. 117–129.

Man, O., 2008. On the identification of magnetostratigraphic polarity zones. Studia Geophysica et Geodaetica 52, 173–186.

Man, O., 2011. The maximum likelihood dating of magnetostratigraphic sections. Geophysical Journal International 185 (1), 133–143.

Métivier, F., Gaudemer, Y., Tapponnier, P., Klein, M., 1999. Mass accumulation rates in asia during the cenozoic. Geophysical Journal International 137 (2), 280–318.

Myers, C. S., Rabiner, L. R., 1981. Comparative study of several dynamic time-warping algorithms for connected-word recognition. The Bell System Technical Journal 60 (7), 1389–1409.

Patriat, P., Achache, J., 1984. India-eurasia collision chronology has implications for crustal shortening and driving mechanism of plates. Nature 311 (5987), 615–621.

Sen, S., Valet, J.-P., Ioakim, C., 1986. Magnetostratigraphy and biostratigraphy of the neogene deposits of Kastellios Hill (Central Crete, Greece). Palaeogeography, Palaeoclimatology, Palaeoecology 53 (2-4), 321–334.

Smith, T. F., Waterman, M. S., 1980. New stratigraphic correlation techniques. Journal of Geology 88 (4), 451–457.

Tapponnier, P., Molnar, P., 1979. Active faulting and Cenozoic tectonics of the Tien Shan, Mongolia, and Baykal region. Journal of Geophysical Research 84 (B7), 3425–3459.

Tauxe, L., Gallet, Y., 1991. A jackknife for magnetostratigraphy. Geophysical Research Letters 18 (9), 1783–1786.

Tauxe, L., Steindorf, J., Harris, A., 2006. Depositional remanent magnetization: Toward an improved theoretical and experimental foundation. Earth and Planetary Science Letters 244 (3-4), 515–529.

Wand, M., Jones, M., 1995. Kernel smoothing. Monographs on statistics and applied probability. Chapman & Hall, London, UK.

Wang, X., Wang, B., Qiu, Z., Xie, G., Xie, J., Will, D.and Qiu, Z., Deng, T., 2003. Danghe area (western Gansu, China) biostratigraphy and implications for depositional history and tectonics of northern Tibetan Plateau. Earth and Planetary Science Letters 208 (3-4), 253–269.

Waterman, M. S., Raymond Jr., R., 1987. The match game: New stratigraphic correlation algorithms. Mathematical Geology 19 (2), 109–127.

Windley, B., Allen, M., Zhang, C., Zhao, Z., Wang, G., 1990. Paleozoic accretion and cenozoic redeformation of the Chinese Tien Shan range, Central Asia. Geology 18 (2), 128–131.

Yin, A., Rumelhart, P., Butler, R., Cowgill, E., Harrison, T. M., Foster, D. A., Ingersoll, R. V., Zhang, Q., Zhou, X.-Q., Wang, X.-F., Hanson, A., Raza, A., 2002. Tectonic history of the Altyn Tagh fault system in northern Tibet inferred from Cenozoic sedimentation. Bulletin of the Geological Society of America 114 (10), 1257–1295.